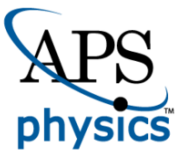

Superradiance and Subradiance due to Quantum Interference of Entangled Free Electrons

Aviv Karnieli, Nicholas Rivera, Ady Arie, and Ido Kaminer

Phys. Rev. Lett. **127**, 060403 — Published 5 August 2021

DOI: 10.1103/PhysRevLett.127.060403

Superradiance and subradiance due to quantum interference of entangled free electrons

Aviv Karnieli[1], Nicholas Rivera[2], Ady Arie[3] and Ido Kaminer[4,*]

[1]Raymond and Beverly Sackler School of Physics and Astronomy, Tel Aviv University, Ramat Aviv 69978, Tel Aviv, Israel
[2]Department of Physics, Massachusetts Institute of Technology, Cambridge, Massachusetts 02139, USA
[3]School of Electrical Engineering, Fleischman Faculty of Engineering, Tel Aviv University, Tel Aviv 69978, Israel
[4]Department of Electrical Engineering, Technion–Israel Institute of Technology, Haifa 32000, Israel

**corresponding authors: kaminer@technion.ac.il; avivkarnieli@tauex.tau.ac.il*

When multiple quantum emitters radiate, their emission rate may be enhanced or suppressed due to collective interference in a process known as super- or subradiance. Such processes are well-known to occur also in light emission from free electrons, known as coherent cathodoluminescence. Unlike atomic systems, free-electrons have an unbounded energy spectrum, and thus all their emission mechanisms rely on electron recoil, in addition to the classical properties of the dielectric medium. To date, all experimental and theoretical studies of super- and subradiance from free electrons assumed only classical correlations between particles. However, dependence on quantum correlations, such as entanglement between free electrons, has not been studied. Recent advances in coherent-shaping of free-electron wavefunctions motivate the investigation of such quantum regimes of super- and subradiance. In this Letter, we show how a pair of coincident path-entangled electrons can demonstrate either super- or subradiant light emission, depending on the two-particle wavefunction. By choosing different free-electron Bell-states, the spectrum and emission pattern of the light can be reshaped, in a manner that cannot be accounted for by a classical mixed state. We show these results for light emission in any optical medium, and discuss their generalization to many-body quantum states. Our findings suggest that light emission can be sensitive to the explicit quantum state of the emitting matter wave, and possibly serve as a non-destructive measurement scheme for measuring the quantum state of many-body systems.

Collective effects in light emission, such as super (and sub-) radiance are of great importance for intense and coherent light sources. These effects cause the emission by N particles to be enhanced (suppressed) relative to the emission by N independent particles[1,2], and have been studied thoroughly in the context of Dicke superradiance in systems of bound electrons[3–8]. Super- (and sub-) radiance also proves important in the classical domain, when energetic charged particles form bunches and superradiate[9–13] or subradiate[14–16]. Such a process constitutes the basis for technologies such as klystrons, traveling-wave tubes, and free-electron lasers[10,11,17].

In contrast to the super- and subradiance from bound-electrons, which necessitates a quantum theory, super- and subradiance from free electrons (and other charged particles) is well-described classically in all experimental regimes so far[9–13,18]. Even the quantum description of superradiance by multiple free charged particles[19–23] essentially recovered the same predictions as the classical description.

The possibility of strong *quantum* effects in super and subradiance by free-electrons, arising from quantum correlations such as entanglement (Fig. 1a-b), was until now left unexplored. This question is further motivated by recent breakthroughs in the coherent manipulation of free electrons[24–29] (e.g., in electron microscopes) with strong lasers. The laser-driven quantum electrons provide attractive new prospects for controllable quantum sources of light[31-42], due to their continuum of energy states. This difference from bound-electron systems has special importance for creating sources in hard-to-access wavelength regimes[12,41–46], while enjoying ultrafast timescales and nanometric spatial resolution. Most of these new predictions, however, consider only a single quantum electron interacting with quantum light, leaving out potentially rich opportunities for coherent control of photon emission, enabled by several free-electrons.

In this work, we show how quantum correlations between multiple electrons can shape light emission by creating a new effect of quantum super- and sub-radiance. To show this, we develop the general quantum theory of spontaneous emission by a correlated system of free charged particles (detailed in the Supplementary Material), and employ it for the example of Cherenkov radiation by free electrons. For the important case in which the particles are free electrons, the process of light emission is also called coherent cathodoluminescence[47] (CCL). We adopt the acronym CCL below, while keeping in mind that the predictions apply to other charged particles.

To exemplify the general concept of quantum super- and subradiance for multiparticle CCL, we present results for the concrete case of light emission by two path-entangled free electrons. We consider each electron as having a delocalized wavepacket larger than the emitted wavelength. This case naively corresponds to incoherent emission[48] in both the classical and the quantum descriptions. Surprisingly, we find that the emitted light intensity directly depends on the quantum phase angle of the two-electron Bell-state, and that both super- and subradiant light emission can be obtained for different quantum states. This phenomenon has no classical or semiclassical analogue, and is experimentally distinct from emission by free-electron bunches. Our findings have implications on the emerging field of free-electron quantum optics[30,33,38], suggesting that photoemission can be used as a probe of multi-particle emitters[48]. Compared to recent work on light emission from quantum free electrons, our work is the only one to consider *many-body* ensembles and predict novel *quantum* effects.

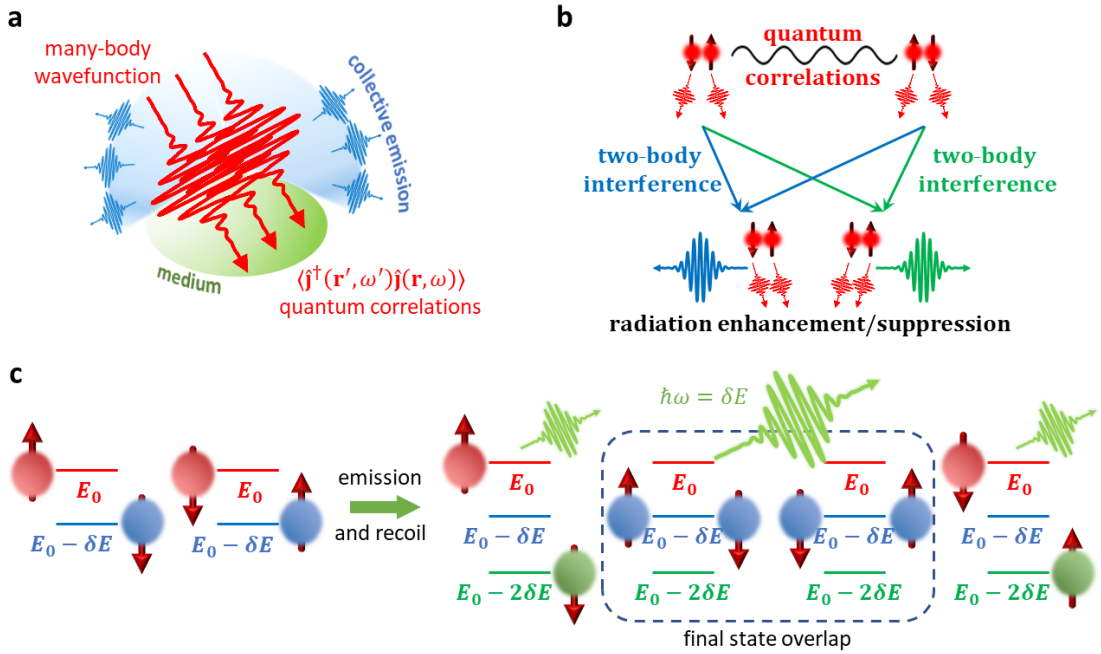

Fig. 1: Super- and subradiance from quantum-correlated free charged particles. (a) A quantum current operator $\hat{\mathbf{j}}(\mathbf{r},t)$, associated with the emission of light quanta by multiple charged particles in a general optical environment, is used to find the collective (super- or subradiant) emission by calculating current-current correlations. (b) Exemplifying the general concept, when a pair of quantum-correlated particles emits radiation, the quantum interference between the transition amplitudes can lead to enhancement or suppression of the emitted light intensity. (c) This system can be realized by two free-electrons of opposite spins with kinetic energy levels spaced by δE, prepared in an entangled state (left). Then, upon emission of a single photon, the 2-electron state recoils by $\hbar\omega = \delta E$. Overlap between recoiled final states results in quantum interference leading to super- and subradiance.

CCL by free charged particles. To illustrate our findings, we consider CCL by free electrons in a general optical environment described by a dyadic Green function[49,50] $\mathbf{G}(\mathbf{r},\mathbf{r}',\omega)$. The initial state of the electron-radiation field is described by a density matrix $\boldsymbol{\rho}_\mathrm{i} = \boldsymbol{\rho}_\mathrm{e} \otimes |0\rangle\langle 0|$, where $\boldsymbol{\rho}_\mathrm{e}$ denotes the initial electron density matrix and $|0\rangle\langle 0|$ denotes the vacuum state of the radiation. The interaction is governed by the Dirac Hamiltonian: $H_\mathrm{int} = ec\boldsymbol{\alpha}\cdot\mathbf{A}$, where e is the electron charge, c is the speed of light, $\boldsymbol{\alpha}^i = \boldsymbol{\gamma}^0\boldsymbol{\gamma}^i$ are the Dirac matrices, and $\mathbf{A}$ is the electromagnetic vector potential operator. We use first-order time-dependent perturbation theory to find the final quantum state of the system, $\boldsymbol{\rho}_\mathrm{f}$.

In CCL experiments, only the radiation field is measured and so we calculate its reduced density matrix, $\boldsymbol{\rho}_\mathrm{ph} = \mathrm{tr}_\mathrm{e}\{\boldsymbol{\rho}_\mathrm{f}\}$, with tr_e denoting the partial trace over the (multi-)electron state. We calculate the power spectrum of the emitted light measured in the far field at a distance r from the source and at direction $\hat{\mathbf{n}}$ (see Supplementary Material Sections S1-S3 for derivation):

$$\frac{d^2P}{d\Omega d\omega} = 2r^2\epsilon_0 c\omega^2\mu_0^2 \int d^3\mathbf{R}d^3\mathbf{R}'\ \mathrm{Tr}\mathbf{G}^\dagger(r\hat{\mathbf{n}},\mathbf{R}',\omega)\mathbf{G}(r\hat{\mathbf{n}},\mathbf{R},\omega)\left\langle \mathbf{j}^\dagger(\mathbf{R}',\omega)\mathbf{j}(\mathbf{R},\omega)\right\rangle_\mathrm{e} \qquad (1)$$

In Eq. 1, Tr denotes a matrix trace $\mathrm{Tr}\,\mathbf{E}^\dagger\mathbf{E} = \sum_\alpha E_\alpha^\dagger E_\alpha$ over the electric field polarization. The quantity $\left\langle \mathbf{j}^\dagger(\mathbf{r}',\omega')\mathbf{j}(\mathbf{r},\omega)\right\rangle_\mathrm{e} = \mathrm{tr}\{\boldsymbol{\rho}_\mathrm{e}\mathbf{j}^\dagger\mathbf{j}\}$ is the expectation value, with respect to the *electronic initial state*, of the correlations in the current density operator $\mathbf{j}(\mathbf{r},t) = ec\hat{\boldsymbol{\psi}}^\dagger\boldsymbol{\alpha}\hat{\boldsymbol{\psi}}$,

where $\widehat{\boldsymbol{\psi}}(\mathbf{r},t)$ [defined in Eq. (S2.10)] is the electron spinor field operator described in second quantization.

We now make the two following simplifications: (i) the particles propagate as wavepackets with a well-defined carrier velocity $\mathbf{v}_0$ (equivalent to the paraxial approximation, where the electron dispersion is linearized); (ii) photon-induced recoil associated with the momentum $\hbar q$ are much smaller than electron momenta p_e (under this approximation, recoil is assumed small but is not neglected). These assumptions are applicable to a vast number of effects, including all cases in which the emitter is relativistic and for all free-electron sources in the microwave, radio frequency and optical ranges[42,44,47,51,52]. The current correlations appearing in Eq. 1 can then be written as (see Supplementary Material Section S2 for derivation)

$$\langle \mathbf{j}(\mathbf{x}')\mathbf{j}(\mathbf{x})\rangle = e^2\mathbf{v}_0\mathbf{v}_0\left[G_\mathrm{e}^{(2)}(\mathbf{x}',\mathbf{x}) + \delta(\mathbf{x}-\mathbf{x}')G_\mathrm{e}^{(1)}(\mathbf{x},\mathbf{x})\right], \tag{2}$$

where $\mathbf{x} = \mathbf{r} - \mathbf{v}_0 t$ and $\mathbf{x}' = \mathbf{r}' - \mathbf{v}_0 t'$. In Eq. (2), we define the first- and second-order correlation functions of the emitter $G_\mathrm{e}^{(1)}(\mathbf{x}',\mathbf{x}) = \sum_\sigma \mathrm{tr}\{\boldsymbol{\rho}_\mathrm{e}\hat{\psi}_\sigma^\dagger(\mathbf{x}')\hat{\psi}_\sigma(\mathbf{x})\}$ and $G_\mathrm{e}^{(2)}(\mathbf{x}',\mathbf{x}) = \sum_{\sigma'}\sum_\sigma \mathrm{tr}\{\boldsymbol{\rho}_\mathrm{e}\hat{\psi}_{\sigma'}^\dagger(\mathbf{x}')\hat{\psi}_\sigma^\dagger(\mathbf{x})\hat{\psi}_\sigma(\mathbf{x})\hat{\psi}_{\sigma'}(\mathbf{x}')\}$, respectively, where $\hat{\psi}_\sigma(\mathbf{x})$ are position-space annihilation operators corresponding to the particle spin components $\sigma = \uparrow,\downarrow$ (under our approximations, these scalar operators are decoupled from their vector spinors, see Eq. (S2.15)). Eq. 2 is valid for particles with both fermionic and bosonic statistics. The current correlation of Eq. (2) comprises two terms: a pair correlation term proportional to $G_\mathrm{e}^{(2)}(\mathbf{x}',\mathbf{x})$, giving rise to coherent radiation when substituted into Eq. (1); and a term proportional to the probability density $G_\mathrm{e}^{(1)}(\mathbf{x},\mathbf{x})$, contributing incoherent radiation[48].

Quantum super- and subradiance by free charged particles. The quantum interference of the multiparticle free-electron wavefunction with itself can leave an imprint on the spontaneously-emitted light. Such quantum features are sensitive to the specific quantum state the system was prepared in and cannot be accounted for by classical electromagnetism. Here, we shall consider the enhancement (suppression) of radiation emission above (below) the rate of independent free electrons as super- (sub-) radiance, as commonly employed in the literature for CCL[53,54], although other definitions exist for atomic systems (mainly categorized by the initial pumping conditions)[55]. The quantum interference phenomenon considered here originates from the second-order correlation between the emitting particles, $G_\mathrm{e}^{(2)}(\mathbf{x},\mathbf{x}')$ in Eq. (2), which determines the emission pattern in Eq. (1). We consider the decomposition

$$G_\mathrm{e}^{(2)}(\mathbf{x},\mathbf{x}') = G_\mathrm{e}^{(1)}(\mathbf{x},\mathbf{x})G_\mathrm{e}^{(1)}(\mathbf{x}',\mathbf{x}')g_\mathrm{e}^{(2)}(\mathbf{x}-\mathbf{x}'). \tag{3}$$

where $g_\mathrm{e}^{(2)}(\mathbf{x}-\mathbf{x}')$ now stands for the normalized second-order correlation function of the emitting particles. It is worth mentioning that from Eqs. (1-3), the known semiclassical cases of superradiance could be recovered. For example, radiation from subwavelength-bunched beams[9], regularly-spaced bunches (as in the bunching effect in FELs[17]), and sub-shot noise resulting from Coulomb interactions[14–16]. In such cases, the spatio-temporal shape of the multiparticle wavefunction determines the power spectrum.

In the following, however, we shall focus on the case where $g_\mathrm{e}^{(2)}(\mathbf{x}-\mathbf{x}')$ is determined by *quantum correlations* rather than classical correlations. As a proof-of-concept, we consider a two-electron state prepared from two identical, delocalized wavepackets $\varphi(\mathbf{x})$ having two

possible carrier momenta: $\mathbf{k}, \mathbf{k}'$ and different spins ↑, ↓, as can be created in a Stern–Gerlach-type experiment (or other techniques of spin polarization[56]). Note that the spin degree of freedom, while usually insignificant for first-order spontaneous emission, becomes important here for the preparation of an entangled free-electron state. The electron pair traverses coincidentally through a general optical medium and spontaneously emits CCL radiation, as illustrated in Fig. (2a-b). We assume that the wavefunction momentum uncertainty around $\mathbf{k}, \mathbf{k}'$ is smaller than the difference $|\mathbf{k} - \mathbf{k}'|$, ensuring that the two states initially do not overlap in momentum space.

Further, we assume that spatio-temporal walk-off (or group velocity mismatch) between the two wavepackets is negligible. This can be readily assured for electrons whenever $\mathbf{k} - \mathbf{k}'$ is of the order of optical momenta, and the wavefunction spatial extent in the respective dimension along $\mathbf{k} - \mathbf{k}'$ is larger than the optical wavelength. Under these assumptions, it can be easily shown [see Eq. (S4.1-2)] that the two wavepackets occupied by each of the electrons are $e^{+i(\mathbf{\Delta k}/2)\cdot\mathbf{x}}\varphi(\mathbf{x})$ and $e^{-i(\mathbf{\Delta k}/2)\cdot\mathbf{x}}\varphi(\mathbf{x})$, where $\varphi(\mathbf{x})$ has a carrier wavenumber $\mathbf{k}_0 = (\mathbf{k} + \mathbf{k}')/2$, and where $\mathbf{\Delta k} = \mathbf{k} - \mathbf{k}'$.

The key idea is to allow one electron with wavevector $\mathbf{k}$ to emit a photon with wavevector $\mathbf{q}$, and get recoiled to a new wavefunction centered near $\mathbf{k}'$. We want this new recoiled wavefunction to overlap with the wavefunction of a *second* electron already occupying $\mathbf{k}'$ (assuming the two electrons have opposite spins). Quantum interference between two equivalent photon emission paths then happens if we interchange the two electrons (see Fig. 1).

We illustrate the emission from classically-correlated electrons in Fig. 2a and quantum-correlated electrons in Fig. 2b. For the classical case, we consider *probabilistic* correlations. If one electron is found in state $\mathbf{k}$ ↑, it is correlated with the other to be found in $\mathbf{k}'$ ↓, and vice versa. This corresponds to the mixed state $\rho_\mathrm{e} = 1/2|\mathbf{k}_\uparrow\mathbf{k}'_\downarrow\rangle\langle\mathbf{k}_\uparrow\mathbf{k}'_\downarrow| + 1/2|\mathbf{k}_\downarrow\mathbf{k}'_\uparrow\rangle\langle\mathbf{k}_\downarrow\mathbf{k}'_\uparrow|$. From Eqs. (1-3), one may calculate the power spectrum $d^2P/d\Omega d\omega = \hbar\omega\Gamma(\hat{\mathbf{n}}, \omega)$ of the classically-correlated state, where $\Gamma(\hat{\mathbf{n}}, \omega)$ is the emission rate per unit time per unit frequency. For the classical case, $G_\mathrm{e}^{(1)} = 2|\varphi(\mathbf{x})|^2$, and $g_\mathrm{e}^{(2)}(\mathbf{x} - \mathbf{x}') = 1/2$. We denote the resulting classical emission rate by $\Gamma_\mathrm{c}(\hat{\mathbf{n}}, \omega)$ and the single-particle emission by Γ_0. We find an incoherent emission, i.e. $\Gamma_\mathrm{c} = N\Gamma_0$ (with $N = 2$ in our case), for wavelengths smaller than the extent of the wavepacket $|\varphi(\mathbf{x})|^2$. We also find the expected classical superradiance, i.e. $\Gamma_\mathrm{c} = N^2\Gamma_0$, for wavelengths larger than the extent of the wavepacket. See Fig. 2d for an example.

In the quantum case, we may consider a *fundamentally* different correlation, e.g., an entanglement between an electron pair prepared in a path-entangled Bell-state: $|\Psi\rangle = \left(|\mathbf{k}_\uparrow; \mathbf{k}'_\downarrow\rangle + e^{i\zeta}|\mathbf{k}_\downarrow; \mathbf{k}'_\uparrow\rangle\right)/\sqrt{2}$, where ζ is a phase angle. It is readily shown that in this case, we have again $G_\mathrm{e}^{(1)} = 2|\varphi(\mathbf{x})|^2$, whereas

$$g_\mathrm{e}^{(2)}(\mathbf{x} - \mathbf{x}') = \frac{1}{2}(1 - \cos\zeta\cos[\Delta\mathbf{k}\cdot(\mathbf{x} - \mathbf{x}')]). \tag{4}$$

Unlike the classical case of $g_\mathrm{e}^{(2)} = 1/2$, the quantum case in Eq. (4) depends explicitly on the quantum phase angle ζ of the electron Bell-state, and on the wavevector difference $\Delta\mathbf{k} = \mathbf{k} - \mathbf{k}'$. Calculating the quantum emission rate Γ_q from Eqs. (1-3) and (4) gives the general result

$$\Gamma_\mathrm{q} = \Gamma_\mathrm{c} - \cos\zeta\,\Gamma_{\Delta\mathbf{k}}, \tag{5}$$

where $\Gamma_{\Delta\mathbf{k}}$ is a term resulting from the momentum difference $\Delta\mathbf{k}$ of the two modes $\mathbf{k}$ and $\mathbf{k}'$. This term can influence the radiated spectrum by shifting the long wavelength superradiance peak in momentum space to shorter wavelengths (Fig. 2d). This property, together with the control over the quantum phase angle ζ, allows for selective **enhancement or suppression of the emission rate at wavelengths that exhibit no super- or subradiance in the classical picture**: i.e., we find a peak (or dip) in the emission intensity that cannot be explained by spatial modulation (bunching) of the density cloud $G_{\mathrm{e}}^{(1)} = 2|\varphi(\mathbf{x})|^2$ (the two chosen wavepacket modes $e^{+i(\Delta\mathbf{k}/2)\cdot\mathbf{x}}\varphi(\mathbf{x})$ and $e^{-i(\Delta\mathbf{k}/2)\cdot\mathbf{x}}\varphi(\mathbf{x})$ differ only by phase and are not modulated in amplitude). Therefore, Eq. (5) introduces a *quantum* radiation effect that is sensitive to the quantum correlation between electrons and shows how they induce strong enhancement or suppression of spontaneous emission.

Note that the phase dependent term, $\cos\zeta$ of Eq. (5) – the quantum interference in superradiance and subradiance – happens *independently* of any temporal delay effects between electrons, as previously analyzed in the literature[19,20]. In fact, the radiation phenomenon we described does not rely on the localization of the wavefunction to dimensions smaller than the emitted wavelengths, nor on temporal separation between electrons (see Supplementary Material Section S5).

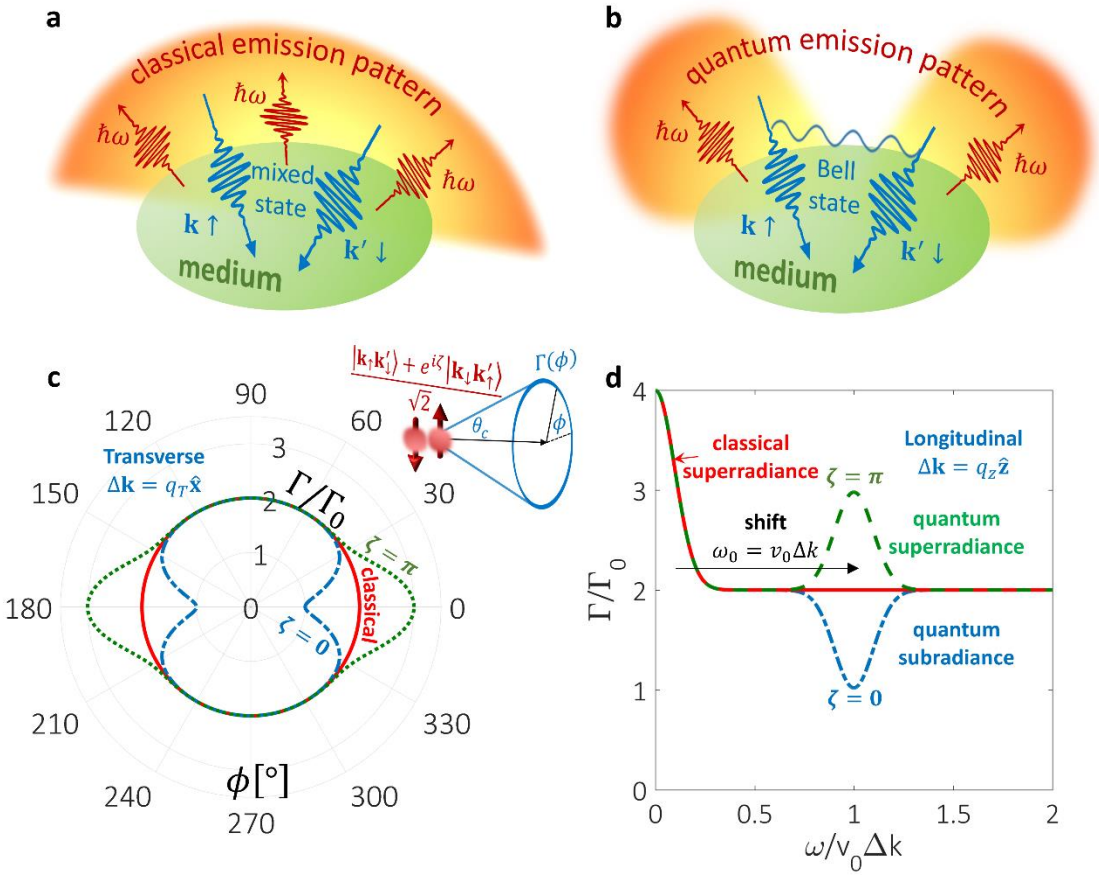

Figure 2: Shaping light using quantum correlations. (a-b) Illustration of coherent cathodoluminescence from two correlated particles. In (a), a pair of coincident electrons with different momenta $\mathbf{k}, \mathbf{k}'$ and spins ↑↓ are prepared in a classically correlated (mixed) state and interact with an optical environment – giving classical emission. In (b), the electrons are instead prepared in a path-entangled Bell-state, and the emission pattern is modified, depending explicitly on the phase angle ζ of the electrons' quantum state. (c-d) Quantum shaping of Cherenkov radiation by two-electron Bell-states. **(c)** The rate of Cherenkov photon emission per unit time per unit frequency Γ, normalized by the single-particle rate $\Gamma_0 = \alpha\beta\sin^2\theta_c/2\pi$. The normalized rate Γ/Γ_0 is calculated along the Cherenkov cone

and plotted as a function of the azimuthal angle ϕ (see inset). For different phases ζ of the electron Bell-state, the radiation pattern is no longer azimuthally symmetric on the cone as in the classical case (red full line), and is either enhanced ($\zeta = \pi$, green dotted line) or suppressed ($\zeta = 0$, blue dashed-dotted line). The wavepackets that constitute the two-electron Bell-state differ by a transverse wavevector $\Delta\mathbf{k} = \sin\theta_c\, n\omega/c\hat{\mathbf{x}} = q_T\hat{\mathbf{x}}$, chosen to match the transverse photon momentum q_T. **(d)** Normalized emission rate Γ/Γ_0 vs. normalized frequency in units of $\omega_0 = v_0\Delta k$, where now $\Delta\mathbf{k}$ is chosen parallel to $\hat{\mathbf{z}}$. Near $\omega = v_0\Delta k = \omega_0$, a resonance appears. The magnitude of the spectral feature is governed by the phase angle ζ of the Bell-state, giving quantum super- and subradiance. Electron velocity $v_0 = 0.7c$, refractive index $n = 2$, emitted photon energy $\hbar\omega = 2$ eV, wavefunction dimensions in (c) $\Delta r_T = 200$ nm and $\Delta z = 1$ nm and in (d) $\Delta r_T = 10$ nm and $\Delta z = 500$ nm, for the transverse and longitudinal sizes, respectively.

Cherenkov radiation. As an example of our findings, we consider Cherenkov radiation (CR), observed when a charged particle of velocity $v = \beta c$ surpasses the phase velocity of light in a homogeneous dielectric medium of refractive index $n = n(\omega)$. CR is known to have a broad spectrum, and is characterized by a cone-shaped emission pattern, where the aperture of the cone is determined by the Cherenkov angle $\theta_C = \arccos(1/n\beta)$. For the two-electron cases discussed above, the CR emission rate is found using Eqs. (1-5), yielding

$$\Gamma(\hat{\mathbf{n}},\omega) = \frac{\alpha\beta}{2\pi}\sin^2\theta\,\delta\left(\cos\theta - \frac{1}{n\beta}\right)\Bigg\{\underbrace{2 + 2\left|\int d^3\mathbf{x}\, e^{-i\frac{n\omega}{c}\hat{\mathbf{n}}\cdot\mathbf{x}}|\varphi(\mathbf{x})|^2\right|^2}_{\text{classical}} - \underbrace{\cos\zeta\left[\left|\int d^3\mathbf{x}\, e^{-i\left(\frac{n\omega}{c}\hat{\mathbf{n}}-\Delta\mathbf{k}\right)\cdot\mathbf{x}}|\varphi(\mathbf{x})|^2\right|^2 + \Delta\mathbf{k}\leftrightarrow-\Delta\mathbf{k}\right]}_{\text{quantum}}\Bigg\}, \tag{6}$$

In Eq. (6), note that the first two terms correspond to the classically-correlated state (giving the classical emission rate Γ_c), while the third term appears only for the quantum-correlated electron Bell-state of phase angle ζ, with $\Gamma_{\Delta\mathbf{k}}$ proportional to the shifted Fourier transform of the wavepacket. The shifted spectrum, together with the phase angle ζ, can be used to tailor quantum super- and subradiant CR.

Fig. 2c-d illustrates this example using two choices of $\Delta\mathbf{k}$: matching the transverse momentum (Fig. 2c) or the longitudinal momentum (Fig. 2d) of the emitted CR photon in a specific optical wavelength. For the quantum-correlated case, this matching results in a shaped emission pattern and spectrum at the chosen wavelength. The quantum phase angle ζ controls, in the transverse case (Fig. 2c), the quantum suppression and enhancement of the radiation with respect to the classical emission rate in opposite angles on the Cherenkov cone. Similarly, in the longitudinal case (Fig. 2d) the phase ζ induces super- and subradiance at the chosen resonant frequency ω_0 that is matched to the momentum difference via $\omega_0 = v_0\Delta k$.

It is noteworthy to compare this result to Dicke superradiance[1,2] in systems of atomic emitters. For example, consider the super- and subradiance of two stationary atoms. The entanglement of the form $(|eg\rangle + e^{i\zeta}|ge\rangle)/\sqrt{2}$, where e (g) stands for an excited (ground) state of the atom, can lead to super- and subradiance[57]. Different regimes of super- and subradiance in the presence of atomic center-of-mass motions were also recently investigated[58,59], showing that atomic recoil tends to diminish collective emission (i.e., beyond the Lamb-Dicke regime[58,59]). However, recoil plays a different role in atomic and free-electron systems. In the known regimes of atomic superradiance, the internal electronic transition is what mainly determines the properties of the emitted light (e.g. its frequency and polarization), with the atomic recoil being a secondary effect. For free-electrons, the recoil is the main emission

mechanism, defining (together with the properties of the dielectric medium and the initial electron energy) the emitted wavelength through energy conservation of the free-electron transition. Surprisingly, the recoil in the free-electron system is found to be the key ingredient for quantum super- and subradiance.

Generalization to N particles. So far we considered two emitters only, but our results can be readily applied to the case of many-body states of free charged particles, by the choice of appropriate wavefunctions of the form

$$|\Psi\rangle = \sum_{\{\sigma_1\sigma_2\ldots\sigma_N\}} c_{\{\sigma_1\sigma_2\ldots\sigma_N\}}|\varphi_1\sigma_1, \varphi_2\sigma_2, \ldots, \varphi_N\sigma_N\rangle, \tag{7}$$

where σ_i is the spin of particle i occupying the wavepacket $\varphi_i(\mathbf{r})$. Even for the much-higher dimensionality of the wavefunction, the same current correlations of Eq. 2 enable deriving observables as above. When the number of particles grows, entanglement features and Pauli exclusion[60] play an increasingly important role in the shaping of radiation patterns. Looking forward, it is extremely interesting to find which many-body states create macroscopic states of light that widely differ from conventional types of light emission and from classical super- and subradiance. Such findings could serve as concrete evidence for the breakdown of the correspondence principle[61] between Maxwell's equations and quantum electrodynamics.

Experimental considerations. Path entangled free electron states were observed in double photoionization from H_2 molecules[62,63]. Other directions for entangled electrons have been proposed by exploiting the interactions of free electrons with cavity photons[33,64]. The phase angle of these states could be controlled using path differences[65] or through interaction with an optical field[28]. In addition, spectral modulation of two (or more) entangled electron states can be implemented using photon-induced electron microscopy (PINEM) techniques[26].

We emphasize that the quantum interference exists even in the complete absence of classical interference effects, such as those related to inducing a space charge modulation or time delay between the two electrons. This point is shown in the Supplementary Material Section S5, for any wavepacket shape and for any optical medium. Consequently, our entangled-driven super- and subradiance can enable a clear experimental signature of quantum super- and subradiance from entangled particles.

We investigate the decoherence of the two-electron quantum state following the emission of an optical excitation in an arbitrary environment (Supplemental Material Section S6). We find that although the final state becomes partially mixed, quantum correlations persist in the form of *recoiled* copies of the initial quantum state (see Eqs. S6.4a-b). Excitations with small recoil relative to the electronic momentum uncertainty lead to very small decoherence (Eq. S6.6). In this context, optical setups such as cavities[24,25] or aloof geometry experiments[66] can be employed to completely avoid decoherence from sample excitations other than the desired emitted photons. Finally, we show that the interaction between the optical environment and the two-electron wavefunction can be employed to create the necessary two-electron entanglement[33,64] that we consider in this work; the entanglement can be created by virtue of post-selecting an emitted photon (see Eq. S6.9 and Fig. S1).

In summary, we unveiled the role of quantum correlations in enabling a novel form of super- and subradiance from several free charged particles. This effect was previously analyzed only in the presence of classical correlations. Harnessing the quantum interference between two

path-entangled electrons, we showed how the intensity pattern and spectrum of CCL, and generally of any emission process from charged particles, can be selectively enhanced or suppressed, depending on the quantum state of the particles. The center-of-mass recoil plays an essential role in such processes, in contrast to what is currently known in atomic quantum optics. Therefore, we expect this new insight to stimulate the discovery of novel superradiance regimes in other areas of quantum optics, and particularly in atomic physics.

Our findings pave the way towards novel methods for ultrafast quantum coherent control of light emission using quantum correlated wavefunctions on the attosecond timescale[26], complementing existing schemes of controlling photons by atomic emitters[67]. The unbound energy spectrum of free particles enables a larger volume of quantum information to be carried by them[68]. By considering super- and subradiance by entangled free-electron energy ladders[69], multiple optical harmonics can be enhanced or suppressed. The emitted photons can take the form of a quantum frequency comb[70], enabling a large bandwidth of quantum communication.

Looking at the bigger picture, our results suggest that any form of wave emission by free particles could serve for passive and non-destructive quantum measurement[71] of the entanglement between the emitting particles. The prospects of such a detection scheme are due to the detection not requiring the absorption of the particles in a detector, allowing further use of the quantum system after the measurement.

The predictions can be generalized to any type of correlated free particles interacting with any type of wave quanta, for example: Bose-Einstein condensate systems interacting with superfluid Bogoliubov excitations[72], spontaneous parametric downconversion from macroscopic quantum states of light[73], and in condensed matter, excitations of polaritonic quasiparticles[51] by both free electrons[47] and bound conduction electrons[74].

We first presented the results that led to this work in the CLEO conference in May 2020[75]*.*

References

1. Gross, M. & Haroche, S. Superradiance: An essay on the theory of collective spontaneous emission. *Phys. Rep.* **93**, 301–396 (1982).
2. Dicke, R. H. Coherence in spontaneous radiation processes. *Phys. Rev.* **93**, 99–110 (1954).
3. Guerin, W., Araújo, M. O. & Kaiser, R. Subradiance in a Large Cloud of Cold Atoms. *Phys. Rev. Lett.* **116**, 083601 (2016).
4. Goban, A. *et al.* Superradiance for Atoms Trapped along a Photonic Crystal Waveguide. *Phys. Rev. Lett.* **115**, 063601 (2015).
5. Scheibner, M. *et al.* Superradiance of quantum dots. *Nat. Phys.* **3**, 106–110 (2007).
6. Bienaimé, T., Piovella, N. & Kaiser, R. Controlled Dicke subradiance from a large cloud of two-level systems. *Phys. Rev. Lett.* **108**, 123602 (2012).
7. Jahnke, F. *et al.* Giant photon bunching, superradiant pulse emission and excitation trapping in quantum-dot nanolasers. *Nat. Commun.* **7**, 11540 (2016).
8. Solano, P., Barberis-Blostein, P., Fatemi, F. K., Orozco, L. A. & Rolston, S. L. Super-radiance reveals infinite-range dipole interactions through a nanofiber. *Nat. Commun.* **8**, 1–7 (2017).

9. Gover, A. *et al.* Superradiant and stimulated-superradiant emission of bunched electron beams. *Rev. Mod. Phys.* **91**, (2019).

10. Bostedt, C. *et al.* Linac Coherent Light Source: The first five years. *Rev. Mod. Phys.* **88**, 015007 (2016).

11. Pellegrini, C., Marinelli, A. & Reiche, S. The physics of x-ray free-electron lasers. *Rev. Mod. Phys.* **88**, 015006 (2016).

12. Korbly, S. E., Kesar, A. S., Sirigiri, J. R. & Temkin, R. J. Observation of Frequency-Locked Coherent Terahertz Smith-Purcell Radiation. *Phys. Rev. Lett.* **94**, 054803 (2005).

13. Cook, A. M. *et al.* Observation of Narrow-Band Terahertz Coherent Cherenkov Radiation from a Cylindrical Dielectric-Lined Waveguide. *Phys. Rev. Lett.* **103**, 095003 (2009).

14. Ratner, D., Hemsing, E., Gover, † A, Marinelli, A. & Nause, A. Subradiant spontaneous undulator emission through collective suppression of shot noise. *Phys. Rev. Spec. Top. - Accel. Beams* **18**, 050703 (2015).

15. Gover, A., Nause, A., Dyunin, E. & Fedurin, M. Beating the shot-noise limit. *Nat. Phys.* **8**, 877–880 (2012).

16. Ratner, D. & Stupakov, G. Observation of shot noise suppression at optical wavelengths in a relativistic electron beam. *Phys. Rev. Lett.* **109**, 034801 (2012).

17. O'Shea, P. G. & Freund, H. P. Free-electron lasers: Status and applications. *Science* vol. 292 1853–1858 (2001).

18. Hirschmugl, C. J., Sagurton, M. & Williams, G. P. Multiparticle coherence calculations for synchrotron-radiation emission. *Phys. Rev. A* **44**, 1316–1320 (1991).

19. García De Abajo, F. J. & Giulio, V. Di. Quantum and Classical Effects in Sample Excitations by Electron Beams. *arXiv:2010.13510* (2020).

20. Angioi, A. & Piazza, A. Di. Quantum Limitation to the Coherent Emission of Accelerated Charges. *Phys. Rev. Lett.* **121**, (2018).

21. Kling, P., Giese, E., Carmesin, C. M., Sauerbrey, R. & Schleich, W. P. High-gain quantum free-electron laser: Emergence and exponential gain. *Phys. Rev. A* **99**, 053823 (2019).

22. Peter Kling, Enno Giese, Rainer Endrich, Paul Preiss, Roland Sauerbrey, W. P. S. What defines the quantum regime of the free-electron laser? *New J. Phys.* **17**, 123019 (2015).

23. Robb, G. R. M. & Bonifacio, R. Coherent and spontaneous emission in the quantum free electron laser. *Phys. Plasmas* **19**, 073101 (2012).

24. Kfir, O. *et al.* Controlling free electrons with optical whispering-gallery modes. *Nature* **582**, 46–49 (2020).

25. Wang, K. *et al.* Coherent interaction between free electrons and a photonic cavity. *Nature* **582**, 50–54 (2020).

26. Priebe, K. E. *et al.* Attosecond electron pulse trains and quantum state reconstruction in ultrafast transmission electron microscopy. *Nat. Photonics* **11**, 793–797 (2017).

27. Feist, A. *et al.* Quantum coherent optical phase modulation in an ultrafast transmission electron microscope. *Nature* **521**, 200–203 (2015).

28. Echternkamp, K. E., Feist, A., Schäfer, S. & Ropers, C. Ramsey-type phase control of free-electron beams. *Nat. Phys.* **12**, 1000–1004 (2016).

29. Krüger, M., Schenk, M. & Hommelhoff, P. Attosecond control of electrons emitted from a nanoscale metal tip. *Nature* **475**, 78–81 (2011).

30. Di Giulio, V., Kociak, M. & de Abajo, F. J. G. Probing quantum optical excitations with fast electrons. *Optica* **6**, 1524 (2019).

31. Giulio, V. Di & de Abajo, F. J. G. Free-Electron Shaping Using Quantum Light. *Optica* vol. 7 1820–1830 (2020).

32. Murdia, C. *et al. Controlling light emission with electron wave interference*. https://arxiv.org/pdf/1712.04529.pdf.

33. Kfir, O. Entanglements of Electrons and Cavity Photons in the Strong-Coupling Regime. *Phys. Rev. Lett.* **123**, 103602 (2019).

34. Bendaña, X., Polman, A. & García De Abajo, F. J. Single-photon generation by electron beams. *Nano Lett.* **11**, 5099–5103 (2011).

35. Gover, A. & Yariv, A. Free-Electron-Bound-Electron Resonant Interaction. *Phys. Rev. Lett.* **124**, 064801 (2020).

36. Zhao, Z., Sun, X.-Q. & Fan, S. Quantum entanglement and modulation enhancement of free-electron-bound-electron interaction. *arXiv:2010.11396* (2020).

37. Gover, A. *et al.* Resonant Interaction of Modulation-correlated Quantum Electron Wavepackets with Bound Electron States. (2020).

38. Hayun, A. Ben *et al.* Shaping Quantum Photonic States Using Free Electrons. *arXiv:2011.01315* (2020).

39. Gorlach, A. *et al.* Ultrafast non-destructive measurement of the quantum state of light using free electrons. (2020).

40. Karnieli, A., Rivera, N., Arie, A. & Kaminer, I. Light emission is fundamentally tied to the quantum coherence of the emitting particle. (2020).

41. Remez, R. *et al.* Spectral and spatial shaping of Smith-Purcell radiation. *Phys. Rev. A* **96**, 061801 (2017).

42. Polman, A., Kociak, M. & García de Abajo, F. J. Electron-beam spectroscopy for nanophotonics. *Nat. Mater.* **18**, 1158–1171 (2019).

43. Shentcis, M. *et al.* Tunable free-electron X-ray radiation from van der Waals materials. *Nat. Photonics* **14**, 686–692 (2020).

44. Adamo, G. *et al.* Light well: A tunable free-electron light source on a chip. *Phys. Rev. Lett.* **103**, 113901 (2009).

45. Pan, Y. & Gover, A. Spontaneous and stimulated emissions of a preformed quantum free-electron wave function. *Phys. Rev. A* **99**, 052107 (2019).

46. Mcneil, B. W. J. & Thompson, N. R. X-ray free-electron lasers. *Nature Photonics* vol. 4 814–821 (2010).

47. García de Abajo, F. J. Optical excitations in electron microscopy. *Rev. Mod. Phys.* **82**, 209–275 (2010).

48. Remez, R. *et al.* Observing the Quantum Wave Nature of Free Electrons through Spontaneous Emission. *Phys. Rev. Lett.* **123**, 060401 (2019).

49. Novotny, L. & Hecht, B. *Principles of nano-optics*. *Principles of Nano-Optics* (Cambridge University Press, 2006).

50. Scheel, S. & Buhmann, S. Y. Macroscopic QED - concepts and applications. *Acta Phys. Slovaca* **58**, 675 (2008).

51. Rivera, N. & Kaminer, I. Light–matter interactions with photonic quasiparticles. *Nature Reviews Physics* vol. 2 538–561 (2020).

52. Charles Roques-Carmes, Steven E. Kooi, Yi Yang, Aviram Massuda, Phillip D. Keathley, Aun Zaidi, Yujia Yang, John D. Joannopoulos, Karl K. Berggren, I. K. & M. S. Towards integrated tunable all-silicon free-electron light sources. *Nat. Commun.* **10**, 3176 (2019).

53. Gover, A. *et al.* Superradiant and stimulated-superradiant emission of bunched electron beams. *Rev. Mod. Phys.* **91**, 035003 (2019).

54. García de Abajo, F. J. & Di Giulio, V. Optical Excitations with Electron Beams: Challenges and Opportunities. *ACS Photonics* **17**, 36 (2021).

55. Kocharovsky, V. V, Zheleznyakov, V. V, Kocharovskaya, E. R. & Kocharovsky, V. V. Superradiance: the principles of generation and implementation in lasers * Related content. *Physics-Uspekhi* **60**, 345 (2017).

56. Karimi, E., Marrucci, L., Grillo, V. & Santamato, E. Spin-to-orbital angular momentum conversion and spin-polarization filtering in electron beams. *Phys. Rev. Lett.* **108**, 044801 (2012).

57. Devoe, R. G. & Brewer, R. G. Observation of Superradiant and Subradiant Spontaneous Emission of Two Trapped Ions. *Phys. Rev. Lett.* **76**, 2049 (1996).

58. Damanet, F., Braun, D. & Martin, J. Cooperative spontaneous emission from indistinguishable atoms in arbitrary motional quantum states. *Phys. Rev. A* **94**, 33838 (2016).

59. Damanet, F., Braun, D. & Martin, J. Master equation for collective spontaneous emission with quantized atomic motion. *Phys. Rev. A* **93**, 22124 (2016).

60. Rom, T. *et al.* Free fermion antibunching in a degenerate atomic Fermi gas released from an optical lattice. *Nature* **444**, 733–736 (2006).

61. Bohr, N. & Nielsen, J. R. *The correspondence principle : 1918-1923*. (North-Holland Pub. Co, 1976).

62. Akoury, D. *et al.* The simplest double slit: Interference and entanglement in double photoionization of H2. *Science (80-.).* **318**, 949–952 (2007).

63. Waitz, M. *et al.* Two-Particle Interference of Electron Pairs on a Molecular Level. *Phys. Rev. Lett.* **117**, 083002 (2016).

64. Mechel, C. *et al.* Imaging the collapse of electron wave-functions: the relation to plasmonic losses. in *Conference on Lasers and Electro-Optics (2019), paper FF3M.6*

FF3M.6 (The Optical Society, 2019).

65. Lichte, H. & Lehmann, M. Electron holography—basics and applications. *Reports Prog. Phys.* **71**, 016102 (2008).

66. Dahan, R. *et al.* Resonant phase-matching between a light wave and a free-electron wavefunction. *Nat. Phys.* **16**, 1123–1131 (2020).

67. Lu, J., Zhou, L., Kuang, L. M. & Nori, F. Single-photon router: Coherent control of multichannel scattering for single photons with quantum interferences. *Phys. Rev. A - At. Mol. Opt. Phys.* **89**, 013805 (2014).

68. Reinhardt, O., Mechel, C., Lynch, M. & Kaminer, I. *Free-Electron Qubits*.

69. Barwick, B., Flannigan, D. J. & Zewail, A. H. Photon-induced near-field electron microscopy. *Nature* **462**, 902–906 (2009).

70. Kues, M. *et al.* Quantum optical microcombs. *Nat. Photonics* **13**, 170–179 (2019).

71. Reiserer, A., Ritter, S. & Rempe, G. Nondestructive detection of an optical photon. *Science (80-.).* **342**, 1349–1351 (2013).

72. Carusotto, I., Hu, S. X., Collins, L. A. & Smerzi, A. Bogoliubov-Cerenkov radiation in a Bose-Einstein condensate flowing against an obstacle. *Phys. Rev. Lett.* **97**, (2006).

73. Agafonov, I. N., Chekhova, M. V. & Leuchs, G. Two-color bright squeezed vacuum. *Phys. Rev. A - At. Mol. Opt. Phys.* **82**, 011801 (2010).

74. Kaminer, I. *et al.* Efficient plasmonic emission by the quantum ÄŒ erenkov effect from hot carriers in graphene. *Nat. Commun.* **7**, (2016).

75. Karnieli, A., Rivera, N., Arie, A. & Kaminer, I. Coneference talk: Unveiling Emitter Wavefunction Size via the Quantum Coherence of its Radiation. *Conference on Lasers and Electro-Optics (May 2020)* FTu3D.5 https://osa.zoom.us/rec/play/YNzAU7COMEQOWVKHnYEFqriGAy_kaV7kCHoiRh22NXLxtZfpdwRI3F3o8GRvQFR_JCBg0nWwkaMjFLnk.KUdmeKsaWritaj9d?continueMode=true&_x_zm_rtaid=5qoJm4GnRPmk0y-XPZPKNQ.1603880501651.f698ab76cabac4272ad6465ec6fc32ce&_x_zm_rhtaid=259.